



HAL
open science

Water solubility in silica and quartzofeldspathic melts

François Holtz, Jacques Roux, Harald Behrens, Michel Pichavant

► **To cite this version:**

François Holtz, Jacques Roux, Harald Behrens, Michel Pichavant. Water solubility in silica and quartzofeldspathic melts. *The American Mineralogist*, 2000, 85, pp.682-686. hal-00077547

HAL Id: hal-00077547

<https://insu.hal.science/hal-00077547>

Submitted on 31 May 2006

HAL is a multi-disciplinary open access archive for the deposit and dissemination of scientific research documents, whether they are published or not. The documents may come from teaching and research institutions in France or abroad, or from public or private research centers.

L'archive ouverte pluridisciplinaire **HAL**, est destinée au dépôt et à la diffusion de documents scientifiques de niveau recherche, publiés ou non, émanant des établissements d'enseignement et de recherche français ou étrangers, des laboratoires publics ou privés.

Water solubility in silica and quartzofeldspathic melts

FRANCOIS HOLTZ,^{1,2,*} JACQUES ROUX,¹ HARALD BEHRENS,² AND MICHEL PICHAVANT¹

¹ Centre de Recherches sur la Synthèse et la Chimie des Minéraux, CRSCM-CNRS, 1A rue de la Férellerie, 45071 Orléans, France

² Institut für Mineralogie, Universität Hannover, Welfengarten 1, 30167 Hannover, Germany

ABSTRACT

Water solubility in silica melts was determined at 100–600 MPa, 1200–1350 °C, and at each temperature (T) was found to increase with pressure (P). At $P \leq 250$ MPa, the effect of T on water solubility in silica melts is small and within analytical precision (± 0.15 wt% H₂O). A positive correlation with T was observed at 400 MPa. Increasing solubility of water with increasing T was observed when large amounts of water are dissolved in silica and quartzofeldspathic melts (i.e., when molecular water is the dominant species in the glasses at room temperature), as already observed for feldspar melts. Change in water solubility (expressed in mol%) with decreasing SiO₂ content of the melt is nonlinear along the silica-albite join. In the compositional range Ab₁₀₀ to Ab₂₅ (100 to 25 mol% albite, respectively, compositions calculated on an eight-oxygen basis), the solubility of water at 200 MPa decreases only slightly with decreasing Ab content (-0.1 ± 0.01 mol% H₂O per mol% albite). However, at Ab contents less than 25 mol%, water solubility decreases sharply with increasing Qz content. Similar behavior was observed at 500 MPa. These results suggest that two different incorporation mechanisms of water in quartzofeldspathic melts must be considered: one corresponding to an NaAlSi₃O₈-H₂O mechanism, the other to an SiO₂-H₂O mechanism.

INTRODUCTION

Data on water solubility and speciation of water in silica melts are needed to determine the incorporation mechanisms of water in more complex, multicomponent aluminosilicate melts. Although numerous studies have focused on water incorporation mechanisms in aluminosilicate melts of feldspar stoichiometry, very few data are available for the join silica-albite. For albite melts, the NMR results of Kohn et al. (1989) suggested that hydroxyl groups are not bonded to Si. Sykes and Kubicki (1993) suggested that only minor Si-(OH) bonds exist in albite. Although the interpretations of Kohn et al. (1989) and Sykes and Kubicki (1993) are still under debate, significant differences are likely between the incorporation mechanisms of water in albite melts, where Na is involved in the dissolution process, and in silica melts, where water species can only be bonded to Si (e.g., Kohn et al. 1989; Pichavant et al. 1992). Because the incorporation mechanisms of water in pure silica glasses and melts are not fully understood, it is unclear whether models developed for feldspathic melts apply to more silica-rich compositions (e.g., rhyolitic melts).

Experimental data for the SiO₂-H₂O system constrain the H₂O-saturated and H₂O-undersaturated quartz solidus and the solubility of SiO₂ in the fluid phase coexisting with melt or crystals (Ostrovskiy et al. 1959; Kennedy et al. 1962; Stewart

1967; Boettcher 1984). Water solubility data are only available for the pressure (P) and temperature (T) conditions of the SiO₂- and vapor-saturated solidus (Kennedy et al. 1962). Thus, there are no data for hyperliquidus conditions that permit determination of the individual effects of P and T on water solubility. In this study, the solubility of water has been determined for silica melts at 100–600 MPa, 1200–1350 °C, and for albite (Ab) and quartz-albite (Qz-Ab) melts at 200 and 500 MPa, 1100–1300 °C. The data for feldspathic melts constrain the solubility mechanisms of water in intermediate silica-feldspar melt compositions. Numerous studies have been performed to determine water solubilities in albite melts (see review in Behrens 1995; Romano et al. 1996), but little information is available for Qz-Ab melts. The results of Oxtoby and Hamilton (1978a, 1978b) showed that water solubility is significantly higher in quartzofeldspathic melts than in silica melts. However, their data are only qualitative, because water solubility was underestimated at $P > 200$ to 300 MPa due to problems inherent in the analytical technique used to determine the water contents of the glasses (see Silver and Stolper 1989 and Holtz et al. 1995 for further details).

EXPERIMENTAL METHODS AND ANALYTICAL TECHNIQUES

Apparatus and procedures

All experiments to determine the solubility of water in silica melts (Table 1) were conducted at Orléans (CRSCM-CNRS). Experiments with Ab and Qz-Ab compositions were performed

*E-mail: f.holtz@mineralogie.uni-hannover.de

both at Orléans (1300 °C) and Hannover (1200 and 1100 °C). At Orléans, experiments were conducted in two internally heated pressure vessels, oriented vertically and equipped with (kanthal A1 and Pt wound) furnaces as described by Roux et al. (1994). The furnaces permitted samples to be reacted at temperatures as high as 1400 °C for durations up to several days. Thermal gradients along the samples (enclosed in capsules ≤ 2 cm in length) were always less than 10 °C. After switching off furnace power, cooling rates were approximately 300 °C/min between the experimental temperature and 900 °C and 180 to 150 °C/min between 900 and 500 °C. Pressures were measured with transducers, calibrated against a 700 MPa Bourdon-tube gauge (estimated uncertainty: ± 2 MPa). Temperatures were determined using four Pt₉₀Rh₆-Pt₇₀Rh₃₀ unsheathed thermocouples (estimated uncertainty: ± 10 °C). At Hannover, the experiments were conducted in an internally heated pressure vessel oriented vertically and equipped with dual-zone Mo-wound furnaces (estimated uncertainty for pressure: $\pm 0.1\%$ of the measured pressure, see Becker et al. 1998 for further details). Thermal gradients along the samples, measured with four chromel-alumel type K thermocouples (estimated uncertainty: ± 5 °C), were less than 10 °C. Cooling rates were approximately 150 °C/min from experimental temperature down to 500 °C. Cooling from 500 °C to room temperature took approximately 13 to 15 min (for the pressure vessels used at both locations). The starting materials for silica glasses—40 to 200 mg of bubble-free blocks of dry quartzil glass containing a few ppm water and doubly distilled water—were loaded into Pt capsules. Water was added in excess of the expected water solubility

(see Table 1). In some experiments, different fractions of water (all above the expected saturation value) were added to test for the effect of dissolved silica on the water content of the glass. Durations of experiments ranged from 47 to 95 hours (Table 1). The size of the samples and the experimental conditions (P , T , duration) were chosen so that diffusion of water would be sufficiently rapid to achieve a homogeneous distribution of water in the quenched glass samples (see discussion in Holtz et al. 1995). The microprobe analyses of the starting Ab and Qz-Ab anhydrous glasses are given in Holtz et al. (1999). The normative proportions of Qz and Ab (wt% SiO₂ and wt% NaAlSi₃O₈, respectively) in the glasses are: Qz₀:Ab₁₀₀, Qz₂₅:Ab₇₅, Qz₅₀:Ab₅₀, Qz₇₅:Ab₂₅. If the intermediate compositions are expressed as mol% Si₄O₈ and NaAlSi₃O₈, the mole proportions are Qz₂₆Ab₇₄, Qz₅₂Ab₄₈, and Qz₇₆Ab₂₄, respectively.

Determination of water contents

The water contents of the hydrous glasses were determined by Karl Fischer titration (KFT). In this procedure (1) the samples are heated progressively up to 1300 or 1350 °C (for quartzofeldspathic and silica glasses, respectively) in an induction furnace, and (2) the liberated water species are transported by a dry argon stream to a titration cell. The analytical precision increases with increasing amount of sample and is better than ± 0.15 wt% H₂O (the amount of sample used ranged from 10 to 20 mg; for further details on uncertainties, see Behrens 1995; Holtz et al. 1995). Bubble-free glasses were coarsely crushed prior to extraction of water. This was necessary because the sudden release of water in silica-rich glasses can cause them to decrepitate. This lowers measured water contents, because fragments of glass are spewn out of the hot zone of the induction furnace. For bubble-bearing samples, single glass blocks were used to limit loss of water from the quench bubbles during crushing. Further details of this analytical procedure are given by Behrens (1995) and Holtz et al. (1995). Spectroscopic analyses of glasses following KFT showed that the samples still contain 0.10 ± 0.05 wt% H₂O, regardless of the initial water content of the glass or the anhydrous composition (Behrens 1995). Thus, all the measured water contents obtained in this study were corrected by adding 0.1 wt% H₂O. The water solubility data given in Table 1 are average values of all water contents of samples synthesized at the same P and T .

RESULTS

Run products of SiO₂-H₂O samples reacted at $P \leq 250$ MPa were clear, bubble-free glasses, whereas those from samples reacted at $P > 250$ MPa were cloudy, bubble-bearing glasses. In each quenched sample, "free" water was present. In one case (experiment 11, Table 1), the glass was bubble-free at one end of the sample and contained bubbles at the other end. In this experiment, a piece of glass approximately 1 cm long was used, and after reaction it clearly showed that the bubbles were formed during the quench. The explanation for this is as follows. After switching off furnace power, the cooling rates were not uniform in the vertically oriented vessel, and the lower part of the sample cooled faster than the upper part as a result of thermal convection (the temperature gradient was recorded by four ther-

TABLE 1. Experimental conditions for synthesis of hydrous glasses and measured H₂O contents in silica glasses

Caps. no.	P (bars)	T (°C)	H ₂ O added (wt%)	Exp. duration (hours)	Observations	H ₂ O (KFT)	H ₂ O sol. (wt% H ₂ O)
1	1010	1350	5.1	74	C	2.42	2.48
2	1010	1350	8.1	74	C	2.35	
3	1550	1200	5.5	92	C	2.98	3.08
4	1500	1275	6.8	60	C	2.87	3.02
5	1500	1275	14.8	60	C	2.98	
6	1570	1300	6.0	47	C	3.03	3.13
7	1550	1350	6.1	66	C	3.18	3.28
17	2030	1200	6.2	91	C	3.73	3.83
18	2010	1300	6.3	74	C	3.73	3.83
8	2520	1200	8.8	95	QB	4.06	4.25
9	2520	1200	8.5	95	QB	4.24	
10	2500	1280	6.2	62	C	4.02	4.12
11	2520	1350	7.0	90	C/QB	4.35/4.28	4.41
12	4030	1200	8.0	93	QB	5.18	5.32
13	4030	1200	10.0	93	QB	5.26	
14	4100	1350	7.5	59	QB	5.66	5.78
15	4100	1350	12.0	59	QB	5.71	
16	6000	1200	11.0	94	QB	7.95	8.05

Notes: C = clear glass; QB = quench bubbles in the glass.

mocouples). Thus, quenching is faster at the bottom than at the top of a vertically oriented capsule, and the relatively slow quench at the top of the 1 cm long sample explains the presence of bubbles in the upper part of the reacted glass.

The measured water contents of the hydrous silica glasses are given in Table 1, and the effects of P and T on water solubility in these melts are shown in Figure 1. The water solubilities determined in Ab and Qz-Ab melts, as well as in one feldspar melt ($\text{Ab}_{50}\text{Or}_{50}$), are given in Table 2. For these compositions, quench bubbles were not observed in the run products. Table 2 also contains five water solubility values determined at 1100 °C in previous studies.

No significant variation of water content was observed in $\text{SiO}_2\text{-H}_2\text{O}$ glasses reacted at the same P - T conditions (Table 1), and no variation of water content was observed (within analytical error) with changing amount of added water (experiments 4–5 and 12–13, Table 1). The good reproducibility of the experiments, together with the presence of water in each capsule after the experiment and the homogeneous distribution of water within the samples (determined by micro-Raman and micro-infrared spectroscopy), suggest that equilibrium was attained and that the samples were saturated with water. Reversal experiments and duplicate experiments with different run durations were not carried out in this study but were performed by Behrens (1995) with albite glasses reacted at 1100 °C, 200 and 500 MPa. The water contents of the glasses obtained using (1) dry starting material and (2) prehydrated glasses (with initial water contents higher than the expected water solubility) were identical within analytical uncertainty (± 0.11 at 200 MPa and ± 0.14 at 500 MPa). Using glass pieces of the same size as those used in this study, Behrens (1995) showed that the water contents of glasses were identical within analytical uncertainty after run durations of 20 and 100 hours (1100 °C). Because all of the experimental temperatures in this study were above 1100 °C, and run durations were greater than 45 hours (Table 1), we assume that melt-fluid equilibrium was achieved in each of our experiments.

KFT analyses of a bubble-free and a bubble-bearing fragment from the same sample (experiment 11) agree within estimated analytical error, implying that the presence of bubbles

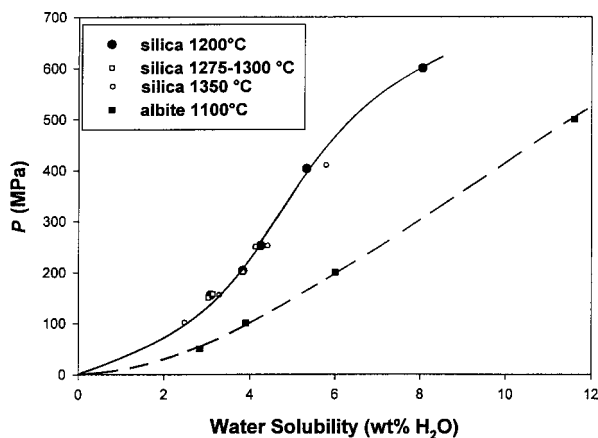


FIGURE 1. Water solubility in silica and albite melts as a function of pressure. Analytical data are presented in Table 1. The continuous curve represents water solubility in silica melts at 1200 °C. A water solubility curve for albite melts at 1100 °C (dashed line, Behrens 1995) is shown for comparison.

has no measurable effect on the determination of water solubility. The micro-Raman spectra of the bubble-free and bubble-bearing parts of the glass obtained in experiment 11 ($P = 252$ MPa) were similar in the frequency range 3000–3700 cm^{-1} , indicating that only minor amounts of water are contained in the bubbles. For glasses with higher water contents (samples synthesized at $P > 400$ MPa), micro-Raman spectra suggest the presence of free water. However, because single glass blocks were used to determine the water contents of bubble-bearing glasses, loss of exsolved water was minimal, and effects on water solubility determinations are probably negligibly small.

The water solubility experiments performed with Ab and Qz-Ab melts were not duplicated. However, the data in Table 2 are internally consistent, and indicate that water solubility is systematically slightly lower at 1300 °C than at 1200 °C, as expected for quartzofeldspathic and alkali feldspar melts at 200 MPa (Holtz et al. 1992; Behrens et al. Unpublished manuscript).

TABLE 2. Water solubility data for feldspathic and quartzofeldspathic melts

Composition	P (bars)	T (°C)	H_2O added (wt%)	Exp. duration (hours)	H_2O sol. (wt% H_2O)	Source of data
Ab_{100}	2030	1200	10.1	91	5.93	this study
Ab_{100}	2010	1300	10.3	74	5.62	this study
$\text{Ab}_{75}\text{Qz}_{25}$	2030	1200	9.9	91	5.57	this study
$\text{Ab}_{75}\text{Qz}_{25}$	2010	1300	10.1	74	5.31	this study
$\text{Ab}_{50}\text{Qz}_{50}$	2030	1200	9.8	91	5.37	this study
$\text{Ab}_{50}\text{Qz}_{50}$	2010	1300	10.5	74	5.10	this study
$\text{Ab}_{25}\text{Qz}_{75}$	2030	1200	10.3	91	4.94	this study
$\text{Ab}_{25}\text{Qz}_{75}$	2010	1300	9.6	74	4.73	this study
$\text{Ab}_{50}\text{Or}_{50}$	2000	1100	9.2 to 10.0	72 to 84	5.68*	Romano et al. (1996)
$\text{Ab}_{38}\text{Qz}_{28}\text{Or}_{34}$	2000	1100	10.0	90	5.41	Holtz et al. (1992)
$\text{Ab}_{29}\text{Qz}_{46}\text{Or}_{25}$	2000	1100	—	—	5.12	extrapolated from Holtz et al. (1992)
$\text{Ab}_{50}\text{Or}_{50}$	5000	1100	10.3	70	10.61	this study
$\text{Ab}_{38}\text{Qz}_{28}\text{Or}_{34}$	5000	1100	20.3	100	10.84	Holtz et al. (1995)
$\text{Ab}_{29}\text{Qz}_{46}\text{Or}_{25}$	5000	1100	—	—	10.30	extrapolated from Holtz et al. (1995)

*Average value from three experiments.

DISCUSSION

Pressure and temperature dependence of water solubility

The effects of pressure and temperature on water solubility in silica melts are shown in Figure 1. The slope of the curve varies with P , and the data obtained at 1200 °C suggest a point of inflection between 300 and 350 MPa. At $P < 300$ MPa, water solubility increases with increasing pressure faster than at $P > 300$ MPa. This behavior is also observed for feldspathic and quartzofeldspathic compositions (see Behrens 1995 and Holtz et al. 1995). In silica melts at $P > 400$ MPa, the rate of increase of water solubility with increasing P becomes more pronounced. This is not observed in albite melts (Fig. 1), and can be attributed to the low pressure at which the upper critical point is attained in the system $\text{SiO}_2\text{-H}_2\text{O}$ (Kennedy et al. 1962). At $P \leq 250$ MPa, the effect of temperature was found to be negligible within experimental and analytical uncertainty. A positive correlation of water solubility with T exists at $P > 250$ MPa (at 400 MPa, water solubility increases by approximately $3 \cdot 10^{-3}$ wt% H_2O per 1°C).

The water solubility data show that the incorporation mechanisms of water in silica melts are different at high and low water contents (Fig. 1). In the pressure range where water solubility is low (i.e., when mainly hydroxyls are incorporated in the melt), water solubility is only slightly affected by changing T (at a given P). In contrast, at a high-water content of the melt (high P), there is a small but significant positive dependence of water solubility on T . A positive temperature dependence of water solubility is also observed at high pressure (500 MPa) in feldspar and quartzofeldspathic melts. At such pressures, significant amounts of molecular water (in addition to hydroxyls) are incorporated into both silica and feldspar melts (e.g., Farnan et al. 1987; Stolper 1982; Nowak and Behrens 1995), leading to the conclusion that the temperature dependence of water solubility is positive when a high proportion of water is dissolved as molecular water in the melts. In contrast, when the dominant species are hydroxyls, the temperature dependence of water solubility is negative (see data of Holtz et al. 1995 and Behrens et al., unpublished manuscript, for 50 and 100 MPa).

Compositional dependence of water solubility and implications

Feldspar melts are known to have higher water solubilities than silica melts at a given P and T . Comparing the solubility of water in silica and albite melts (at 1200 and 1100 °C, respectively) in the range 100–500 MPa shows that water solubility in silica melts, expressed as mol% H_2O on an eight oxygen basis, is approximately 33% lower than that in albite melts (Fig. 1).

The water solubility data can also be used to deduce mechanisms of water dissolution in silica-alkali feldspar melts. In this study, water solubility data was obtained for albite-silica melts at 200 MPa (Table 2). Water solubility data for Ab-Or- H_2O and Ab-Or-Qz- H_2O melts are also available for 200 and 500 MPa from Holtz et al. (1992, 1995), Behrens (1995), and Romano et al. (1996). These data show that water solubility varies nonlinearly with P for compositions along silica-alkali feldspar joins (see Figs. 2 and 3 for compositions along the joins Qz-Ab and Qz-Ab₅₀Or₅₀, respectively). Only small varia-

tions of water solubility are observed for feldspar-rich melts. Decreases in water solubility with increasing Qz content are more pronounced for compositions containing less than 50 mol% feldspar. For Qz-Ab melts at 200 MPa, the data suggest a linear decrease of water solubility with decreasing $\text{NaAlSi}_3\text{O}_8$ content from 100 to 50 mol%. Water solubility starts to decrease significantly with increasing Qz content for compositions containing more than 75 mol% Si_4O_8 . For compositions along the join Qz-Ab₅₀Or₅₀, a linear decrease of water solubility with decreasing feldspar content from 100 to 50 mol% is observed at 200 and 500 MPa (Fig. 3).

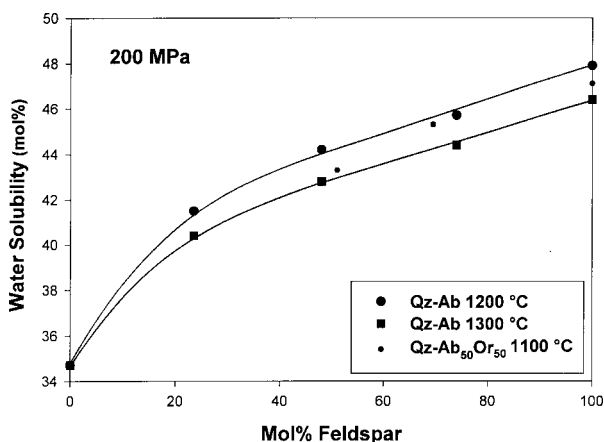


FIGURE 2. Effect of the anhydrous composition of quartzofeldspathic melts on water solubility at 200 MPa. The mole proportion of feldspar component in the anhydrous composition and the water solubility (given in mol% H_2O) are calculated on the basis of eight oxygen atoms/mol silicate. The two water solubility curves are for $\text{Si}_4\text{O}_8\text{-NaAlSi}_3\text{O}_8$ (Qz-Ab) melts at 1200 and 1300 °C. Small dots represent data along the compositional join $\text{Si}_4\text{O}_8\text{-(Na}_{0.5}\text{K}_{0.5})\text{AlSi}_3\text{O}_8$ (composition Qz-Ab₅₀Or₅₀ in the text). The relevant analytical data are given in Tables 1 and 2.

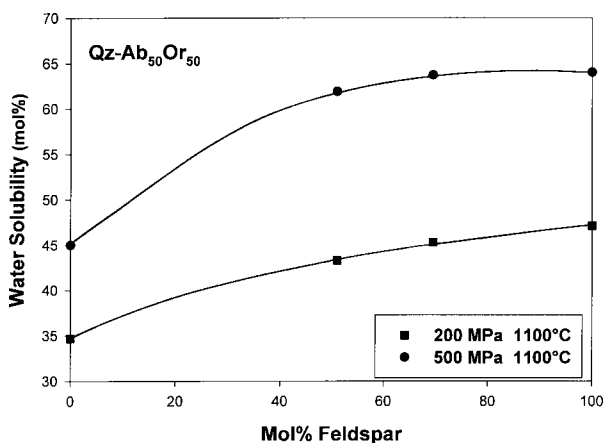


FIGURE 3. Effect of the anhydrous composition of melts along the join $\text{Si}_4\text{O}_8\text{-(Na}_{0.5}\text{K}_{0.5})\text{AlSi}_3\text{O}_8$ on water solubility at 200 and 500 MPa. The mole proportion of feldspar component in the anhydrous composition and the water solubility (given in mol% H_2O) are calculated on the basis of eight oxygen atoms/mol silicate. Data sources: Holtz et al. 1992, 1995; Romano et al. 1996; this study.

The results of this study can be compared with predictions of the water solubility model of Burnham (1979, 1981) and Burnham and Nekvasil (1986). The main observation is that the linear decrease of water solubility (expressed as mol%) with increasing Qz content along the Qz-Ab join, predicted by the thermodynamic model, is incorrect for compositions with high Qz contents (the calculated linear variation of water solubility with Qz content results from the linear change of the Henry's law analog constant as a function of composition, see Holloway and Blank 1994, p. 194–195). The greater solubility of water in feldspar melts than in silica melts suggests that water is preferentially incorporated in melts that contain charge-balancing cations (alkalies). Comparison of water solubilities in pure silica and albite melts suggests that the structural units observed in silica glasses that are composed of corner-sharing SiO₄ tetrahedra (e.g., Konnert et al. 1982; Elliot 1991) can cause a significant decrease in water solubility. Our results suggest that such Na-free structural units only exist in compositions containing between 0 and 50 mol% NaAlSi₃O₈. It is therefore concluded that variations in water solubility along silica-alkali feldspar joins are probably attributable to two different incorporation mechanisms of water. One mechanism is that prevailing in feldspar melts. In the incorporation model for these compositions proposed by Kohn et al. (1989, 1998), water associates with the alkalies to form hydrated Na complexes. The second water solubility mechanism is the same one proposed for silica melts; i.e., depolymerization of the melt and formation of Si-OH bonds (e.g., Stolen and Walrafen 1976; Mysen and Virgo 1986; Farnan et al. 1987). For compositions with albite contents lower than 50 mol%, an interplay between the NaAlSi₃O₈-H₂O mechanism and the SiO₂-H₂O mechanism may control water solubility. The possible existence of two water-solubility mechanisms in such compositions has also been proposed by Schmidt et al. (2000) on the basis of NMR evidence. If the investigated compositions are extrapolated to granitic and rhyolitic melts, the results of this study suggest that the NaAlSi₃O₈-H₂O mechanism predominates in such melts in the pressure range 200–500 MPa. Thus, a complex interaction between two water incorporation mechanisms probably does not need to be considered to model water solubility in natural felsic systems.

ACKNOWLEDGMENTS

This work was supported by Procope (project 96019) and by the EEC TMR network in situ melt properties (project no. ERB FM RX CT 96 00 63). Reviews by J.G. Blencoe and an anonymous reviewer helped us improve this paper.

REFERENCES CITED

- Becker, A., Holtz, F., and Johannes, W. (1998) Liquidus temperatures and phase compositions in the system Qz-Ab-Or at 5 kbar and very low water contents. *Contributions to Mineralogy and Petrology*, 130, 213–224.
- Behrens, H. (1995) Determination of water solubilities in high-viscosity melts: an experimental study on NaAlSi₃O₈ and KAlSi₃O₈ melts. *European Journal of Mineralogy*, 7, 905–920.
- Boettcher, A.L. (1984) The system SiO₂-H₂O-CO₂: melting, solubility mechanisms of carbon, and liquid structure to high pressures. *American Mineralogist*, 69, 823–833.
- Burnham, C.W. (1979) The importance of volatile constituents. In H.S. Yoder, Ed., *The evolution of the igneous rocks*, p. 439–482. Princeton University Press, New Jersey.
- (1981) The nature of multicomponent aluminosilicate melts. *Physics and Chemistry of the Earth*, 13–14, 197–229.
- Burnham, C.W., and Nekvasil, H. (1986) Equilibrium properties of granite pegmatite magmas. *American Mineralogist*, 71, 239–263.
- Elliot, S.R. (1991) Medium-range structural order in covalent amorphous solids. *Nature*, 354, 445–452.
- Farnan, I., Kohn, S.C., and Dupree, R. (1987) A study of the structural role of water in hydrous silica glass using cross-polarisation magic angle spinning NMR. *Geochimica et Cosmochimica Acta*, 51, 2869–2873.
- Holloway, J.R., and Blank, J.G. (1994) Application of experimental results to C-O-H species in natural melts. In *Mineralogical Society of America Reviews in Mineralogy*, 30, 187–230.
- Holtz, F., Behrens, H., Dingwell, D.B., and Taylor, R.P. (1992) Water solubility in aluminosilicate melts of haplogranitic composition at 2 kbar. *Chemical Geology*, 96, 289–302.
- Holtz, F., Behrens, H., Dingwell, D.B., and Johannes, W. (1995) H₂O solubility in haplogranitic melts: compositional, pressure, and temperature dependence. *American Mineralogist*, 80, 94–108.
- Holtz, F., Roux, J., Ohlhorst, S., Behrens, H., and Schulze, F. (1999) The effects of silica and water on the viscosity of hydrous quartzofeldspathic melts. *American Mineralogist*, 84, 27–36.
- Kennedy, G.C., Wasserburg, G.J., Heard, H.C., and Newton, R.C. (1962) The upper three-phase region in the system SiO₂-H₂O. *American Journal of Science*, 260, 501–521.
- Kohn, S.C., Dupree, R., and Smith, M.E. (1989) Proton environments and hydrogen-bonding in hydrous silicate glasses from proton NMR. *Nature*, 337, 539–541.
- Kohn, S.C., Smith, M.E., Dirken, P.J., van Eck, E.R.H., Kentgens, A.P.M., and Dupree, R. (1998) Sodium environments in dry and hydrous albite glasses: improved 1H solid state NMR data and their implications for water dissolution mechanisms. *Geochimica et Cosmochimica Acta*, 62, 79–87.
- Konnert, J., D'Antonio, P., and Karle, J. (1982) Comparison of radial distribution function for silica glass with those for various bonding topologies. *Journal of Non-Crystalline Solids*, 53, 135–141.
- Mysen, B.O. and Virgo, D. (1986) Volatiles in silicate melts at high pressure and temperature. 1. Interaction between OH groups and Si⁴⁺, Al³⁺, Ca²⁺, Na⁺ and H⁺. *Chemical Geology*, 57, 303–331.
- Nowak, M. and Behrens, H. (1995) The speciation of water in granitic glasses and melts determined by in situ near-infrared spectroscopy. *Geochimica et Cosmochimica Acta*, 59, 3445–3450.
- Ostrovskiy, I.A., Mishina, G.P., and Povilaitis, V.M. (1959) Pressure-temperature projection of the system silica-water. *Doklady Akademii Nauk SSSR*, 126, 587–588.
- Oxtoby, S., and Hamilton, D.L. (1978a) The discrete association of water with Na₂O and SiO₂ in NaAl silicate melts. *Contributions to Mineralogy and Petrology*, 66, 185–188.
- (1978b) Calculation of the solubility of water in granitic melts. In W.S. McKenzie, Ed., *Progress in experimental petrology*. Natural Environmental Research Council Publications Series D, no. 11, p. 37–40. Department of Geology, Manchester University, Manchester, U.K.
- Pichavant, M., Holtz, F., and McMillan, P. (1992) Phase relations and compositional dependence of H₂O solubility in quartz-feldspar melts. *Chemical Geology*, 96, 303–320.
- Romano, C., Dingwell, D.B., Behrens, H., and Dolfi, D. (1996) Compositional dependence of H₂O solubility along the joins NaAlSi₃O₈-KAlSi₃O₈, NaAlSi₃O₈-LiAlSi₃O₈, and KAlSi₃O₈-LiAlSi₃O₈. *American Mineralogist*, 81, 452–461.
- Roux, J., Holtz, F., Lefèvre, A., and Schulze, F. (1994) A reliable high-temperature setup for internally heated pressure vessels: applications to silicate melt studies. *American Mineralogist*, 79, 1145–1149.
- Schmidt, B.C., Riemer, T., Kohn, S.C., Behrens, H., and Dupree, R. (2000) Different water solubility mechanisms in hydrous glasses along the Qz-Ab join. Evidence from NMR spectroscopy. *Geochimica et Cosmochimica Acta*, in press.
- Silver, L.A. and Stolper, E.M. (1989) Water in albitic glasses. *Journal of Petrology*, 30, 667–710.
- Stewart, D.B. (1967) Four-phase curve in the system CaAl₂-Si₂O₇-SiO₂-H₂O between 1 and 10 kilobars. *Schweizerische Mineralogische und Petrographische Mitteilungen*, 47/1, 35–59.
- Stolen, R.H. and Walrafen, G.E. (1976) Water and its relation to broken bond defects in fused silica. *Journal of Chemistry and Physics*, 64, 2623–2631.
- Stolper, E. (1982) Water in silicate glasses. an infrared spectroscopic study. *Contributions to Mineralogy and Petrology*, 81, 1–17.
- Sykes, D. and Kubicki, J.D. (1993) A model for H₂O solubility mechanisms in albite melts from infrared spectroscopy and molecular orbital calculations. *Geochimica et Cosmochimica Acta*, 57, 1039–1052.